# FIELD MEASUREMENTS OF SURFACE GAS FLUXES AND SURFACE-WATER CONDITIONS FOR MINE WASTE ROCK MANAGEMENT[1]

L.K. Kabwe[2], G.W. Wilson[3] and J.M. Hendry[4]

**Abstract.** Field measurements of the variations of surface gas fluxes (e.g., $O_2$ and $CO_2$) and waste-rock surface drying and evaporation are critical in the development of a long-term management plan for mine wastes. However, such measurements on waste-rock piles are lacking. Previously, we tested and verified a dynamic closed chamber (DCC) method in minicosms and a mesocosm and then applied at a field-scale to quantify the $CO_2$ efflux at the Key Lake uranium mine, northern Saskatchewan. In this study we investigated the short-term effects of heavy rainfall events on the near surface waste-rock water contents and the resultant $CO_2$ efflux from the Deilmann north waste-rock pile (DNWR). We also investigated the short-term evaporative fluxes using SoilCover numerical model. The corresponding average $O_2$ flux into the pile was estimated using the measured $CO_2$ efflux data and the reported kinetic ratio ($1O_2:0.2CO_2$) determined from samples collected from the DNWR. Using the average value of the measured $CO_2$ efflux (217 mg m$^{-2}$ h$^{-1}$) the corresponding $O_2$ flux into the DNWR was calculated to be 789 mg m$^{-2}$ h$^{-1}$. Results showed that the $CO_2$ gas efflux was dramatically reduced after heavy rainfall events, however, the impart was of relative short duration. This behavior was attributed to hydraulic properties of the waste-rock material. These data can be of value in the long-term development of a plan for mine waste management.

**Additional Key Words**: gas fluxes, waste-rock, unsaturated soil.

# Introduction

Accurate measurements and monitoring of surface gas fluxes (e.g., CO2 and O2) and soil water conditions are needed in the development of a long-term management plan for mine waste dumps. Mine waste-rock piles are, in some cases, constructed upon organic carbon-rich dewatered lake bottoms (Birkham et al., 2003; Lee et al., 2003). Microbial respiration in these buried deposits can consume $O_2$ and produce $CO_2$ (Alexander, 1977; Hass et al., 1983; Thorstenson et al., 1983; Wood and Petraitis, 1984; Solomon and Cerling, 1987; Hendry et al., 1993; Aggarwal et al., 1997; Aggarwal and Dillon, 1998; Birkham et al., 2003). Oxygen consumption and $CO_2$ production by microbial respiration in unsaturated media can be represented by the general reaction:

$$CH_2O + O_2 \rightarrow CO_{2(g)} + H_2O \tag{1}$$
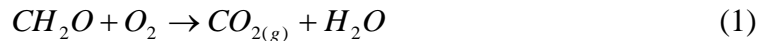
where $CH_2O$ represents a simple carbohydrate. In this simple case of organic oxidation one mole of $O_2$ consumed results in the production of one mole of $CO_2$. More complex organic molecules (e.g., $C_{106}H_{263}O_{110}N_{16}P$) may have molar ratios of $O_2$ consumption to $CO_2$ production of closer to 1:0.77 (Drever, 1997):

$$C_{106}H_{263}O_{110}N_{16}P + 138O_{2(g)} \rightarrow 106CO_{2(g)} + 16NO_3^- + HPO_4^{-2} + 122H_2O + 18H^+ \tag{2}$$
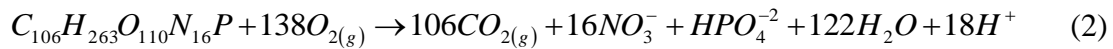
Based on these equations, respiratory consumption of 1 mol of $O_2$ should produce 0.8 or 1 mol of $CO_2$. Lee and co-workers (Lee et al., 2003) found that these stoichiometric ratios are very similar to those observed for microbial respiration in forest soils ($1O_2$:$0.7CO_2$) and in buried lake sediments beneath mine waste-rock piles ($1O_2$:$0.5CO_2$). They found a positive correlation between the rates of $O_2$ consumption and $CO_2$ production and organic carbon content (i.e., higher organic carbon contents in forest soil than lake-bottom sediments) and suggested that the difference in $O_2$/$CO_2$ ratios were due to differences in the stoichiometry of the organic carbon. They also measured the rates of $O_2$ consumption and the corresponding rates of $CO_2$ production in kinetic cells for gneissic waste-rock samples collected from DNWR. A linear relation between the rates of $O_2$ consumption and $CO_2$ production was approximated for the gneissic waste-rock samples with a mean ratio of $1O_2$:$0.2CO_2$. Other researchers (Amundson et al., 1988; Wang et al., 1999) reported positive correlation between respiration rates and organic carbon content in unsaturated zone.

Soil $CO_2$ derived from unsaturated mine waste-rock piles is also produced in abiotic (e.g. sulfide minerals) reactions in situ (Elberling and Nicholson, 1996; Timms and Bennett, 2000; Birkham et al., 2002). If gaseous $O_2$ is present in the unsaturated waste-rock piles, the oxygen can be consumed by microorganisms in the chemical oxidation of minerals (e.g. pyrite) and can lead to formation of acid and sulfate (Ritchie, 1994):

$$FeS_{2(s)} + \frac{7}{2}O_{2(g)} + H_2O \rightarrow Fe^{+2} + 2S_4^{-2} + 2H^+ \tag{3}$$
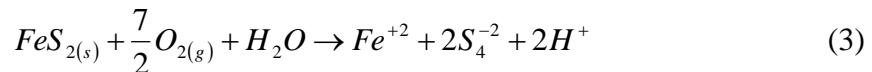
The production of acidic drainage (pollutants) in the pyrite ($FeS_2$) oxidation is dependent on the consumption of $O_2$ (e.g. 2 mol of $H^+$ are produced for every 3.5 mol of oxygen consumed). If, however, there are sufficient carbonate minerals (e.g. calcite $CaCO_3$ or dolomite $CaMg(CO_3)_2$) present, the acid produced in (3) can dissolve available carbon minerals and generate $CO_2$ according to the following reactions (Garrels and Christ, 1965):

$$CaCO_{3(s)} + 2H^+ = Ca^{+2} + H_2CO_3 \qquad (4)$$

$$CaMg(CO_3)_{2(s)} + 4H^+ = Ca^{+2} + Mg^{+2} + 2H_2CO_3 \qquad (5)$$
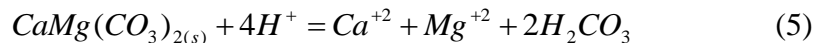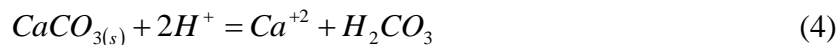
The overall reaction describing the buffering action of carbonate minerals in response to pyrite oxidation is described by reaction (6):

$$FeS_{2(s)} + CaCO_3 + \frac{7}{2}O_{2(g)} \rightarrow Fe^{+2} + Ca^{2+} + 2SO_4^{-2} + CO_{2(g)} \qquad (6)$$
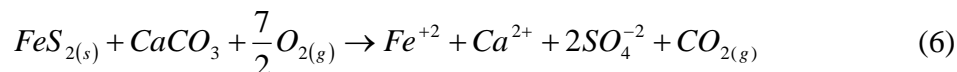
The ratio of 3.5 moles of $O_2$ consumed for every mole of $CO_2$ produced in reaction would also apply if reaction (6) had been written in terms of dolomite instead of calcite. Carbonate buffering of acid generated from sulfide mineral oxidation will typically produce less $CO_2$ than organic oxidation. The $CO_2$ produced is thus an indirect measure for the carbonate buffering and an indicator of the types of oxidation processes occurring. It is therefore suggested that both sulfide oxidation-carbonate buffering and microbial respiration may control $O_2$ and $CO_2$ gas concentrations in the unsaturated waste-rock piles.

Fluctuations in water content due to heavy precipitation events or long drying periods greatly affect the water content profile which affects the gas diffusion and redistribution in the unsaturated zones (Osozawa and Hasegawa, 1995). Measurements of soil surface drying and evaporation are critical since the interface between the surface and atmosphere is the boundary of mass and energy exchanges where the majority of the radiation is absorbed, reflected and emitted; mass is exchanged through evaporation, condensation and precipitation [Gray, 1995]. Precipitation can create changes in soil water content profiles within unsaturated zones, the extent of the effect will depend on the intensity and duration of the rainfall [Freeze, 1969; Capehart and Carlson, 1997]. Prediction of evaporative fluxes under theses conditions is required in the design of soil cover systems. Since the actual rate of evaporation is controlled by both climatic conditions and soil properties, accurate prediction of the actual rate of evaporation from soil surfaces requires a method of analysis that includes both factors.

The objectives of this study were (i) to investigate the short-term effects of heavy rainfall events on the surface and near-surface water contents and the resultant $CO_2$ efflux from the Deilmann north waste-rock pile (DNWR) (ii) to predict short-term evaporative fluxes using SoilCover numerical model following the cessation of rainfall events (iii) to estimate the corresponding $O_2$ flux into the DNWR based on the measured $CO_2$ effluxes (Kabwe et al., 2005b) and the reported kinetic cell ratios for the DNWR (Lee et al., 2003).

## Site Location

The Key Lake uranium mine is located at the southern rim of the Athabasca Basin in north-central Saskatchewan, approximately 750 km north of Saskatoon, Canada ($57^o$ 12' latitude, $105^o$ 35' longitude). Basement rock is unconformably overlain by Athabasca Group sandstone. The sandstone is overlain by sandy glacial deposits. Uranium is associated with the unconformity. Predominant uranium-bearing minerals are $U_2O_7$ and $U_3O_9$ (Key Lake Mining Corporation, 1979). The Deilmann ore body at the Key Lake mine was mined from 1984-1997 (Fig. 1). Many of the lakes within a 5 km radius were drained during pit dewatering and a significant portion of the waste-rock piles were placed directly upon dewatered organic-rich lake-bottom sediments (Richards, 1997).

868

A waste-rock pile, termed the Deilmann north waste-rock pile (DNWR) constructed from overburden sand and gneissic basement rock excavated during open-pit mining of the Deilmann uranium ore body was investigated in this study. The waste-rock pile was constructed in lifts approximately 8 m in height. It has a maximum height of approximately 42 m and a total volume of about 14 million $m^3$.
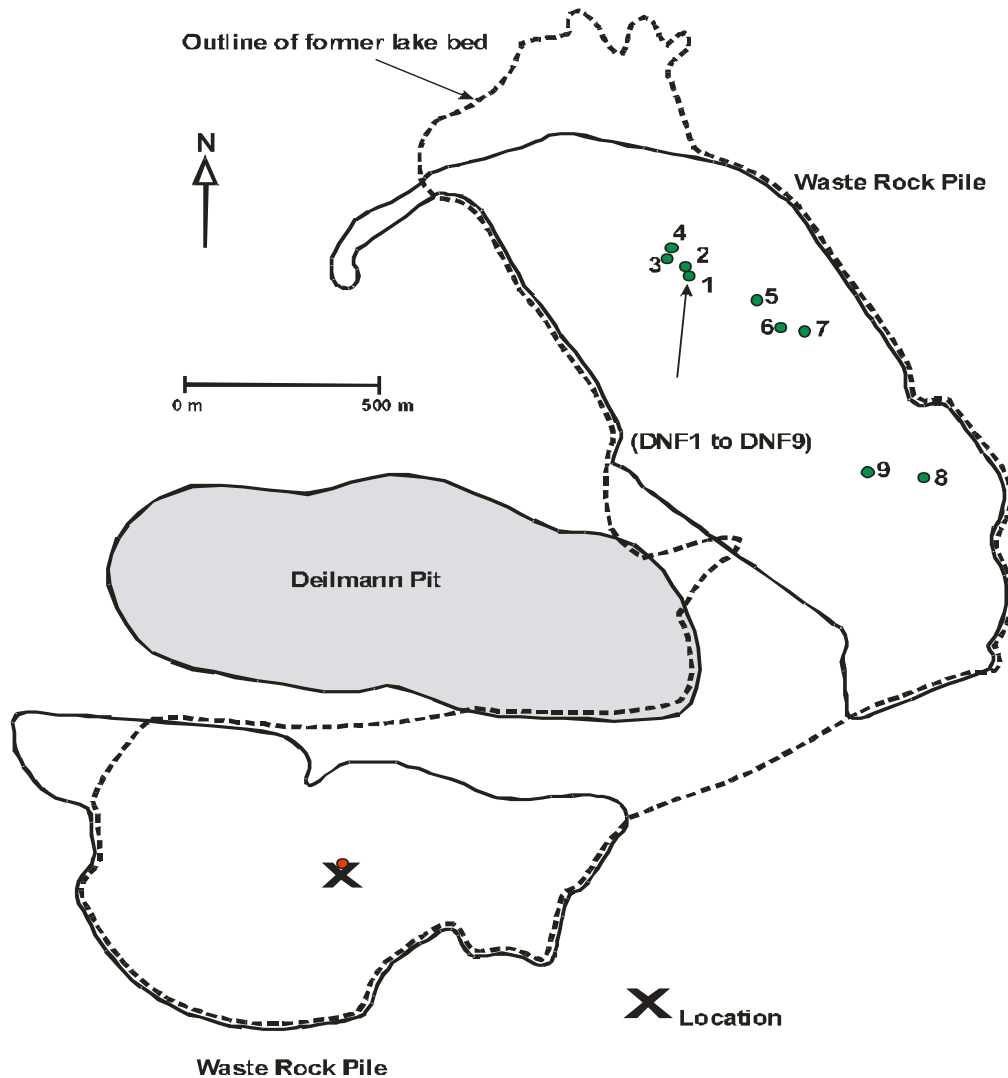


Figure 1.   Site plan of the Deilmann north waste-rock (DNWR) and south waste rock piles (DSWR) and associated Deilmann open pit at Key Lake uranium mine, Saskatchewan, Canada.   The dashed lines outline the extent of lakes drained by mine dewatering. Solid circle represents sampling location; X mark the location of the meteorological weather station.

Haul ramps were used to transport material to each new lift pad where the waste-rock was then dumped and pushed off the edge of the pad to maintain a flat top.   The waste-rock pile consists of approximately 18 m of gneissic basement rock (~10% by volume) overlying

approximately 24 m of sand/sandstone (~90% by volume) from the overburden (Lee et al., 2003). The basement rock in the DNWR generally had larger particles (gravels, boulders and cobbles) compared to sandy waste-rock material.

## Materials and Methods

Grain-size Analysis

A 5-kg sample of weathered waste-rock material from surface and near ground surface (0 to 0.15 m) was collected from DNWR at DF1 (Fig. 1). The grain-size distribution for the sample was determined by sieve analysis. Approximately 200 g of waste-rock sample was dried at 105 $^o$C for 24 h. The oven-dried sample was sieved through sieves with mesh sizes of 4, 10, 20, 40, 60, 80, 100, 140, 200 and 270 on a shaker for 10 min. The mass and percent of waste-rock retained on each sieve were determined by weighing and plotted against the size of the sieve openings.

Soil Water Characteristic Curve (SWCC) Measurement

The SWCC for the waste-rock sample was determined in a Plexiglas$^®$ Tempe cell apparatus (0.1 m diameter. x 0.14 m height) using standard methods (Fredlund and Rahardjo, 1993). In this test, approximately 75 % of the cell volume was filled with the waste-rock sample. The sample was tested using a 1-bar ceramic stone at room temperature of approximately 20 $^o$C. Atmospheric pressure was maintained at the discharge face of the porous stone. After saturation of the waste-rock specimen, increasing pressures of 0.2, 0.5, 1, 2, 3, 4, 5, 6, 7, 8, 9, 10, 20, 50, 80 and 100 kPa were applied to the air phase within the cell. The total mass of the waste-rock filled Tempe cell was monitored continually during the drainage phase of each pressure increment. Equilibrium was achieved when zero discharge (measured as change in mass) was observed over a 24- to 72-h period. When equilibrium at 100 kPa of applied suction was reached, the sample was removed from the Tempe cell. The water content that corresponded to the highest matric suction (100 kPa) was measured by oven drying the waste-rock sample. This water content, together with the previous changes in weight were used to back-calculate the water contents corresponding to the other suction values. The matric suctions were then plotted against their corresponding water contents to yield the SWCC.

Hydraulic Conductivity Measurement

The saturated hydraulic conductivity ($K_s$) of the sample was determined by performing a falling-head hydraulic conductivity test in a stainless steel permeameter cell (0.101 m diameter x 0.116 m height) using an ASTM Standard Test Method, D 5856 (1995). The base and top plates of the permeameter were sealed using rubber O-rings. The top plate was connected to a 100-ml standing pipe burette (0.015 m diameter x 0.70 m height). The base plate was connected to a constant head reservoir. Oven-dried waste-rock sample was uniformly and loosely poured into the cell to about 95 % of the cell volume. The weight of the dry sample was determined by the difference between the weight of the waste-rock-filled cell and the empty cell. The sample was saturated downward with distilled water flowing from the burette through the waste-rock specimen. All air bubbles were removed from the apparatus system by downward flushing of the system with distilled water. A regulated valve was used to allow water from the standing pipe burette to flow through the waste-rock sample. The time for water to fall between two defined elevations on the standing pipe burette was recorded for each test. The test was repeated until a constant time for water to fall a given height was reached. The final sample height was then

measured before the sample was removed from the permeameter cell. The $K_s$ was estimated by a formula (ASTM Standard Test Method, D 5856 (1995)).

The hydraulic conductivity (K) of an unsaturated soil is a function of the degree of saturation (or the volumetric water content) or soil matric suction ($\psi$) (Huang et al., 1998). A number of empirical relationships have been proposed to determine K as a function of volumetric water content or $\psi$ (Richards, 1931; Wind, 1955; Gardner, 1956; Davidson et al., 1969; Philip, 1986; and Ahuja et al., 1988). However, the models proposed by Brooks and Corey (1964) and Mualem (1978) appear to have wider applicability than other models. We used the Brooks and Corey (1964) relation to calculate the unsaturated K.

## Measuring Soil Water Content

The water content for all samples obtained in the field was determined with the gravimetric method. Waste-rock samples were collected at different depths (0, 0.05, 0.10, and 0.15 m) in triplicates of about 100 g each at three different locations around DNF1 (Fig. 1). The samples were placed in zippered airtight plastic bags. Gravimetric water contents were determined by oven drying the waste-rock specimens within 24 h. The replicate measurements were combined to yield a mean water-content value for each depth. The gravimetric water contents were converted to volumetric water contents using data from the SWCC and specific gravity. The waste-rock samples were collected daily during the test period (30 July to 5 August 2002).

## Measuring $CO_2$ Effluxes using the Dynamic Closed Chamber (DCC) System

The DCC flux chambers consist of an open-ended rim (collar) with a lid. Full details of the design, construction, and operation are presented in Kabwe et al. (2002, 2005). Nine collars were installed on the DNWR piles between 27 and 29 April 2000 (Fig. 1). Carbon dioxide analyses were performed using an ADC 2250 differential infrared $CO_2$ gas analyzer (ADC BioScientific Ltd). The analyzer provided simultaneous absolute and differential gas measurements. Full details of the measurements are presented in Kabwe et al. (2002, 2005).

Field studies on short-term effects of rainfall events on soil suction on the DNWR were conducted over an 8-d test period between 29 July and 5 August 2002 at DNF1 (Fig. 1). During this period, a 75.9-mm multi-day rain event (ca. 15% of annual rainfall) fell. The spatial and temporal variations of $CO_2$ effluxes were measured over three time periods in the summer of 2000 (1-11 July, 1-11 August, 8-16 September) (Kabwe et al., 2005b). Similarly, the spatial and temporal variations of $CO_2$ effluxes were measured again over two time periods in the summer of 2002 (13-22 July, 21-26 August) (Kabwe et al., 2005b).

## SoilCover Model

SoilCover (1997) is probably the most widely used code for the design of soil covers for waste-rock dumps and tailings impoundments worldwide (Noel and Rykaart, 2003). SoilCover is a one dimensional finite element package that models transient conditions. The model uses a physically based method for predicting the exchange of water and energy between the atmosphere and a soil surface. SoilCover calculates actual evaporation from a soil profile based on coupled heat and mass flow as governed by the meteoric and soil condition. The theory of SoilCover (1997) is based on the well known principles of Darcy's and Fick's Laws which describe the flow of liquid water and water vapour, and Fourier's Law to describe conductive heat flow in the soil profile below the soil/atmosphere boundary. SoilCover (1997) predicts the evaporative flux from a saturated or an unsaturated soil surface on the basis of atmospheric conditions, vegetation cover, and soil properties. A modified Penman formulation is used to

compute the actual rate of evaporation from the soil/atmosphere boundary (Wilson, 1990 and Wilson et al., 1994):

$$E = \frac{\Gamma Q_n + \eta E_a}{\Gamma + \eta A} \qquad (7)$$

where:

E $\quad$ =Vertical evaporative flux (mm/day)

$\Gamma$ $\quad$ =Slope of the saturation vapour pressure versus temperature curve at the mean temperature of the air

Q $\quad$ =Net radiant energy available at the surface (mm/day)

V $\quad$ =Psychrometric constant

$E_a$ $\quad$ =f(u)$P_a$(B-A)

F(u) $\quad$ =Function dependent on wind speed, surface roughness, and eddy diffusion

$\quad$ =0.35(1+0.1$U_a$)

$U_a$ $\quad$ =Wind speed (km/hr)

$P_a$ $\quad$ =Vapour pressure in the air above the evaporating surface

B $\quad$ =Inverse of the relative humidity of the air=1/ha

A $\quad$ =Inverse of the relative humidity at the soil surface=1/hr

The modified Penman formulation accounts for net radiation, wind speed, and the relative humidity of both the air and soil surface while calculating the actual rate of evaporation (AE) from an unsaturated soil surface. The input requirements for SoilCover are categorized into soil type, climate parameters, vegetation parameters, boundary conditions, initial conditions, and modeling details.

## **Results and Discussion**

Grain-size Analysis
The mean ± one standard deviation envelope of 26 grain-size distributions obtained from the basement-rock core samples from DNWR (Birkham 2002) is presented in Fig. 2 (curves without symbols). The grain-size distribution for the near ground surface (0 - 0.15 m) sample measured in this study (Fig. 2, curve with symbols) was outside the mean ± one standard deviation envelope for the basement-rock core samples. This curve indicated that 83% of the material was sand size with 17% silt- and clay-size particles. The sand sizes ranged from coarse (16%), medium (42%), and fine (25%). The uniformity coefficient ($C_u$) of the sample ($C_u = D_{60}/D_{10}$) was found to be about 6.3 (e.g., $D_{10}$ is the size such that 10% of the particles are smaller than that size). The grain-size distribution could not be considered representative of the entire DNWR pile because boulder-sized particles were excluded from the analysis. Birkham (2002) found that 40% DNWR basement rock bulk sample was cobble-sized. The $C_u$ of the mean grain-size distributions (not shown) for the basement rock was determined to be about 30. This was consistent with the visual observation that basement rock in the DNWR generally had larger particles compared to sand/sandstone material. It should be noted that over the years the exposed

872

rocks have weathered, so that the top surface consists of a silty, sandy soil with a large proportion of rocks below the surface.
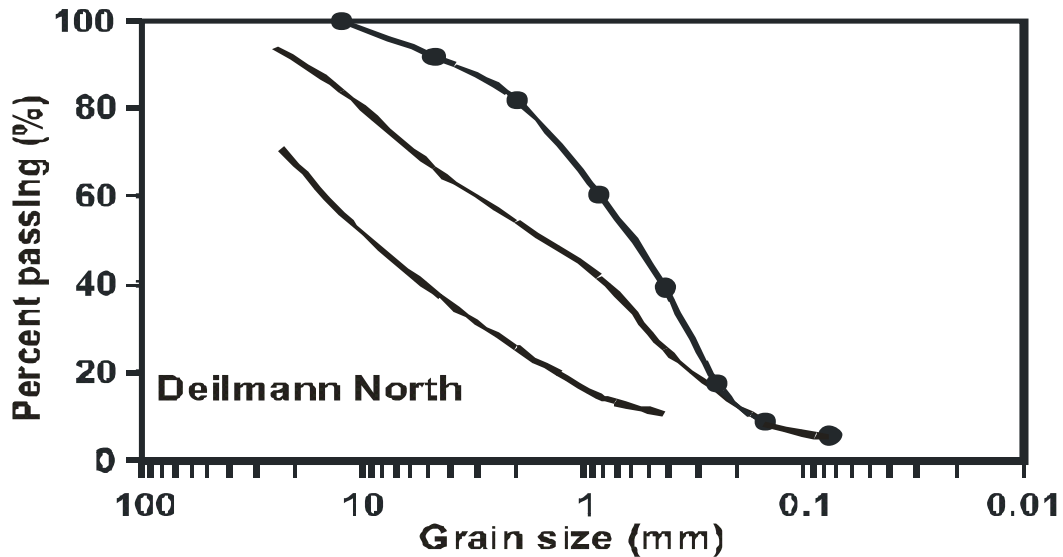


Figure 2.  Particle size distribution curves for the sample of waste-rock from the Deilmann north waste-rock pile (DNWR) for surface sand (curve with symbols) and core basement rock (curves without symbols). Symbols represent measured data from this study. The envelop (curves without symbols) shows the one standard deviation range of grain-size data obtained by Birkman et al. (2002).

Soil Water Characteristic Curve (SWCC)

Figure 3 shows the soil-water characteristic curve (SWCC) for the sample from DNWR determined in the laboratory.  The solid points are measured data and the line represents the best fit curve generated with SoilCover using an equation developed by Fredlund and Xing (1994). The SWCC provides useful information on the water-retention and water-transmission behaviors of piles and help to describe the effects of waste-rock texture and void ratio on the distribution of the water phase in the waste-rock piles and, thus, the gas diffusion in these piles (Barbour, 1998).

In general, the curve is described as having three stages of drying which is well explained in detail in Wilson et al. (1994) and Barbour (1998).  Stage I drying (Fig. 3) is the maximum or potential rate of drying that occurs when the soil surface is or near saturated and is determined by climatic conditions (Wilson et al., 1994).

Stage II drying begins when the conductive properties of the soil no longer permit a sufficient flow of water to the surface to maintain the maximum potential rate of evaporation. Stage III begins when drying rate reaches a slow residual value and the flow of liquid water to the surface ceases and water molecules may only migrate to the surface through the process of vapor diffusion.
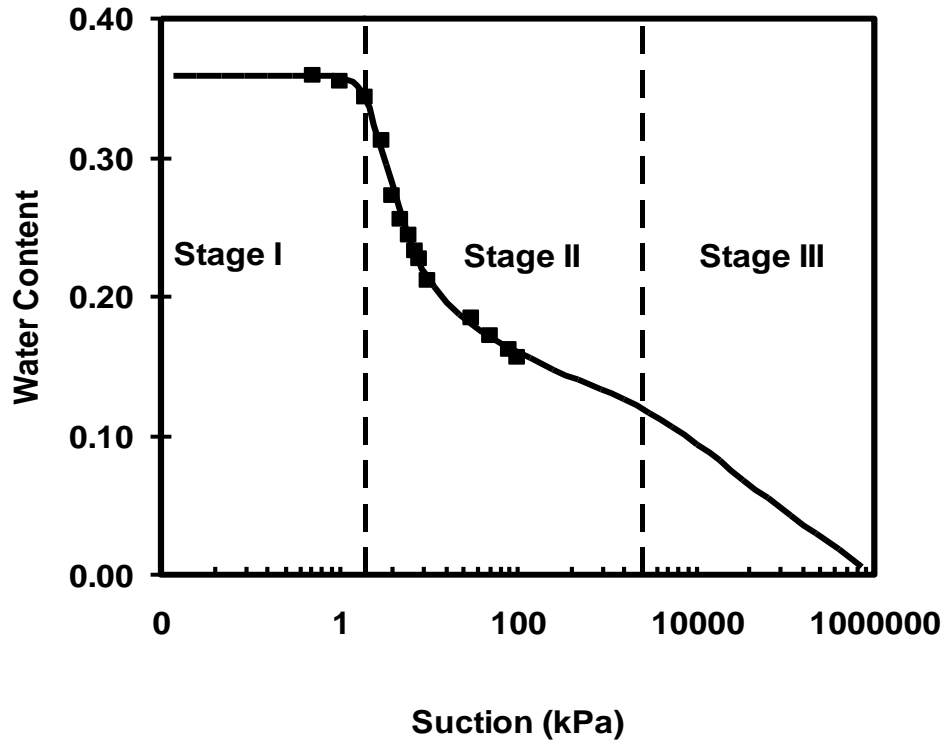
Figure 3.  Soil water characteristic curve (SWCC) of the sample of waste-rock from the Deilmann north waste-rock pile (DNWR). Symbols represent the measured data.

From the SWCC (Fig. 3) the DNWR sample has high volumetric water contents only up to about 2.3 kPa suction, which is the air-entry value (AEV).  The AEV is seen to be the suction at which the soil pores initially filled with water begins to drains.  Because the soil is close to saturation up to 2.3 kPa suction, almost all the pore space is filled with water, and thus the gas fluxes (e.g., $CO_2$ and $O_2$) are expected to be reduced significantly.  It should be noted that the free diffusion coefficient of $CO_2$ is about four orders of magnitude larger in air than in water (Pritchard and Currie 1982); diffusive transport in the water-filled pores is much slower than that in the air-filled voids.  The SWCC shows that the sample drains rapidly between matric suction values of 2.3 and 10 kPa. At 10 kPa suction, the sample retained about 20% water.  This behavior is characteristic of uniform sand-silt materials and has been also described by others (Wilson et al., 1994; Barbour, 1998).

Hydraulic Conductivity (K)

The falling-head tests yielded a value of saturated hydraulic conductivity $K_s$ of $1.20 \times 10^{-6}$ m s$^{-1}$ for the DNWR near ground surface (0-0.15 m) sample.  This value is characteristic of sand and sand-silt materials.  Wilson et al. (1994) obtained similar results for sand from Beaver Creek, Saskatchewan.  The relation between the K and $\psi$ derived from the Brooks and Corey (1964) model for the sample is shown in Fig. 4.  The K of the sample decreased rapidly with increasing $\psi$ past the air-entry value at 2.3 kPa suction.  As suction was increased by two orders of magnitude, the K is predicted to decrease by more than 10 orders of magnitude. At $\psi=100$ kPa, the K value decreased to $<10^{-15}$ m/s.
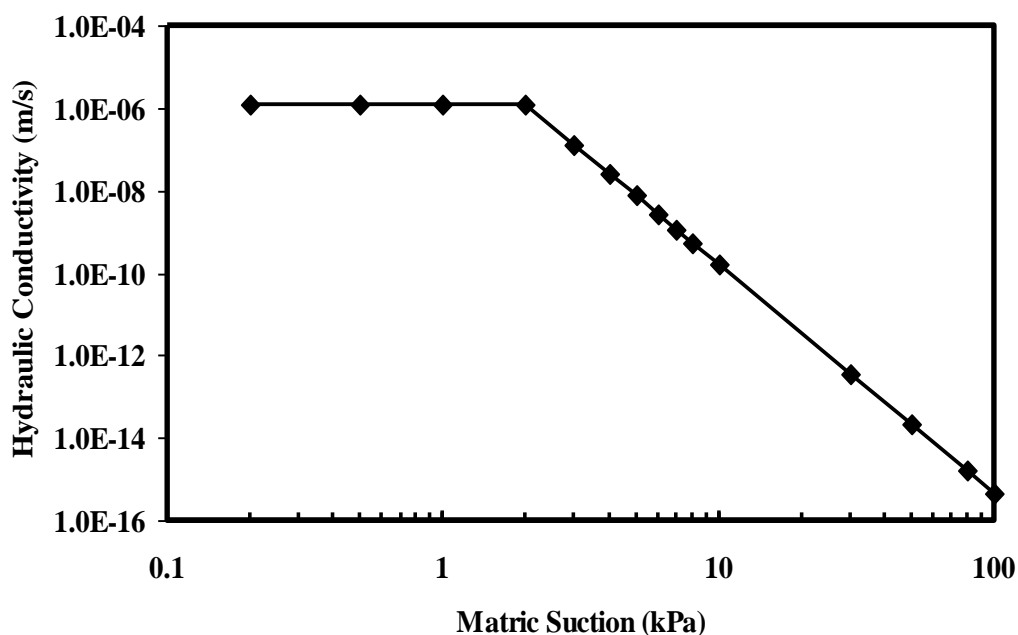
Figure 4.   The unsaturated hydraulic conductivity curve (K) of the sample of waste-rock from the Deilmann north waste-rock pile (DNWR) derived from the Brooks and Corey model.

Measuring $CO_2$ Effluxes and Estimating $O_2$ Fluxes from and into the Deilmann North Waste-Rock Pile  (DNWR)

The surface $CO_2$ flux was measured using a previously calibrated technique in the laboratory (Kabwe et al., 2002) and verified under field conditions (Kabwe et al., 2005).  The spatial and temporal variations of $CO_2$ effluxes were measured over three time periods in the summer of 2000 (1-11 July, 1-11 August, 8-16 September) (Kabwe et al., 2005b).  Similarly, the spatial and temporal variations of $CO_2$ effluxes were measured again over two time periods in the summer of 2002 (13-22 July, 21-26 August) (Table 1 and Fig. 5) (Kabwe et al., 2005b).

The measurements yielded averages $CO_2$ fluxes of $159 \pm 41$ mg $CO_2$ $m^{-2}$ $h^{-1}$, $203 \pm 50$ mg $CO_2$ $m^{-2}$ $h^{-1}$, and $169 \pm 52$ mg $CO_2$ $m^{-2}$ $h^{-1}$ for July, August and September 2000, respectively. Similarly, the measurements yielded averages $CO_2$ fluxes of $302 \pm 83$ mg $CO_2$ $m^{-2}$ $h^{-1}$ and $249 \pm 91$ mg $CO_2$ $m^{-2}$ $h^{-1}$ for July and August, 2002, respectively.  Differences among sampling stations were relatively small (average coefficient of variation (CV) = 32 %)—yielding an overall average flux of $217 \pm 83$ mg $CO_2$ $m^{-2}$ $h^{-1}$ for summers of 2000 and 2002.  However, both calculated mean $CO_2$ effluxes for the summer of 2002 were significantly different from the mean flux calculated for other sampling periods in the summer of 2000.  The cause for the higher measured $CO_2$ flux was not clear at the time of investigation.

Oxygen flux across the surface of the DNWR was not directly measured in this study. Lee et al. (2003) used $O_2$ consumption and $CO_2$ production in kinetic cells to delineate pyrite oxidation-carbonate buffering and microbial respiration in the DNWR. We used the reported kinetic cell ratios (Lee et al. 2003) and the measured $CO_2$ flux in Kabwe et al. (2005b) to estimate $O_2$ flux into DNWR.

Table 1. Summary of results of $CO_2$ efflux measurements using the dynamic closed chamber system (DCC) for the test period of 2000-2002 at Deilmann north waste-rock pile (DNWR) (Kabwe et al., 2005b).

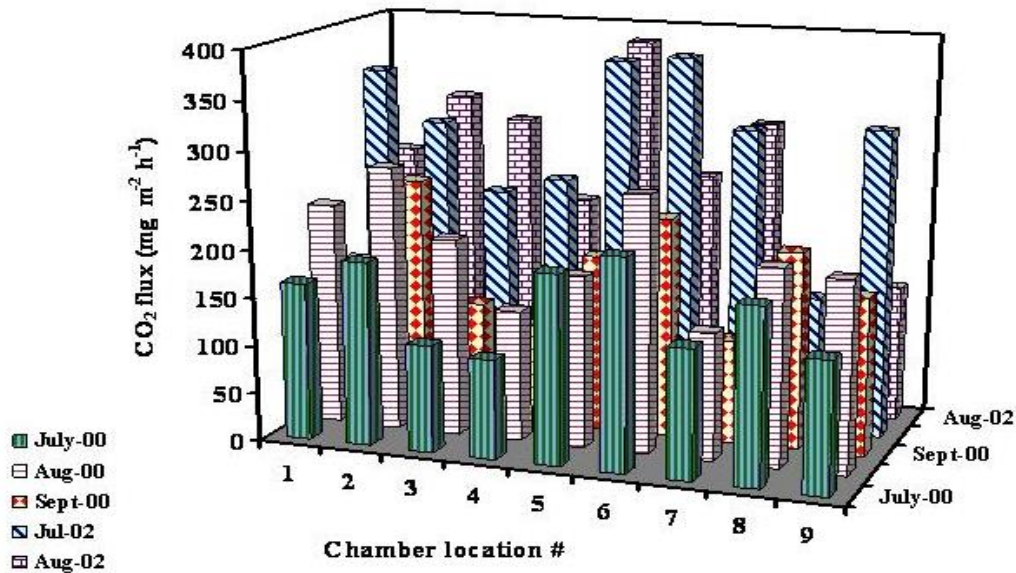| | Summer 2000 | | | Summer 2002 | | |
|---|---|---|---|---|---|---|
| | Mean | Std | CV | Mean | Std | CV |
| | mg m$^{-2}$ h$^{-1}$ | mg m$^{-2}$ h$^{-1}$ | % | mg m$^{-2}$ h$^{-1}$ | mg m$^{-2}$ h$^{-1}$ | % |
| July | 159(n=9) | 41 | 25 | 302(n=9) | 83 | 27 |
| August | 203(n=9) | 50 | 18 | 249(n=9) | 91 | 37 |
| Sept. | 169(n=9) | 52 | 31 | | | |
| Overall | 177 | 50 | 28 | 276 | 89 | 32 |
| Overall average (summer 2000 and summer 2002): | | | ($217 \pm 83$ mg m$^{-2}$ h$^{-1}$) | | | |



Figure 5. Spatial and temporal variations of $CO_2$ effluxes measured over three time periods in the summer of 2000 (1-11 July, 1-11 August, 8-16 September) and again measured over two time periods in the summer of 2002 (13-22 July, 21-26 August).

Based on the kinetic ratio for the gneissic samples from DNWR ($1O_2$:$0.2CO_2$) (Lee et al. 2003) and the overall average measured $CO_2$ efflux from DNWR (217 mg m$^{-2}$ h$^{-2}$) (Kabwe et al., 2005b), the corresponding calculated mean $O_2$ fluxes into DNWR was found to be 789 mg m$^{-2}$ h$^{-2}$. Since the dominant sink for $CO_2$ derived from unsaturated media is the atmosphere and the $CO_2$ in the liquid phase is minor compared to the $CO_2$ flux to the atmosphere, it is valid to assume that the use of $CO_2$ production in the kinetic cells to

characterize microbial respiration and pyrite oxidation-carbonate buffering is conservative (Lee et al., 2003). The observed mean ratio of $1O_2:0.2CO_2$ for gneissic waste-rock was within the range of Eq. 6. Numerous other studies used $CO_2$ production rates to quantify rates of microbial respiration and carbonate buffering in unsaturated geological media Lee et al., 2003; Wood and Petraitis, 1984; Wood et al., 1993; Affek et al., 1998; Keller and Bacon, 1998; Hendry et al., 1999; Grice and Reeve, 1982; Lundgren, 1985; Hendry et al., 1993, 2001; Lawrence and Hendry, 1995; Drake et al., 1996).

Short-term Effects of Rainfall Events on Surface and near Surface-Water Conditions on DNWR

Figure 6 shows the changes of waste-rock water content at and near ground surface (broken lines with open symbols) with time following the cessation of 75.9 mm rainfall (vertical bars) over the initial 48-h period [29 July (day 1) to 30 July, 2002 (day 2)] and the gradual decrease in rainfall from 31 July (day 3) to 2 August (day 5) at the DNWR.

From day 1 to day 2 a total of 75.8 mm of rainfall fell. During this period the soil surface (0 m) was wet in visual appearance on the pile (Fig. 7B) however, the soil water content ($\theta_w$) was not measured on day 1 and day 2. During this wet stage the evaporation is controlled by external meteorological conditions (Hillel 1980, Wilson et al., 1994).

From day 2 to day 3 the rainfall intensity sharply drops from 36.6 mm (day 2) to 7 mm (day 3). The measured soil water at the ground surface (0 m) (broken line with open cicles) was high ($\theta_w \approx 0.25$ or 71% saturation) while water contents at deeper depths (0.05 m – 0.15 m) were relatively lower ($\theta_w \approx 0.15$). At this stage of drying (e.g., beginning of stage II drying process in (Fig. 3), the evaporation rate is limited or dictated by the rate at which the gradually drying soil profile can deliver moisture toward the evaporation zone.

From day 3 to day 5 the rainfall intensity continues to diminish gradually to about 1 mm on day 5. The water content at the ground surface decreased dramatically from 0.25 (day 3) to about 0.03 (day 5) while the water contents at deeper depths (0.10 and 0.15 m) decreased slowly from 0.15 (day 3) to about 0.1 (day 5). As the soil continued to dry a drying layer is being formed at the surface (Wilson et al., 1994) but the rate of actual evaporation is not restricted to suction up to about 3000 kPa.

From day 6 to day 8, there was no rainfall recorded. The ground surface became desiccated ($\theta_w \approx 0.001$) while the water at deeper depths remained elevated. Fig. 8 showed that at higher degree of saturation and during the early stage of drying (e.g., from beginning of saturation measurements, day 1 to day 3), the change of saturation of the surface layer (0 m) and those at deeper depths (0.0 5 – 0.15 m) were proceeding at different rates but more rapidly at the ground surface. As the ground surface became desiccated (from day 4 onward) the changes in saturation of the surface and deeper depths layers started proceeding at approximately the same rates [i.e., the slopes of the lines were similar (-0.010 to -0.015)]. This may signal the transition from stage II to stage III drying when the drying rate reaches a slow residual value. The hydraulic conductivity and the liquid flow at these values of water content are approaching zero. The flow of water to the surface must be predominantly by vapor diffusion.
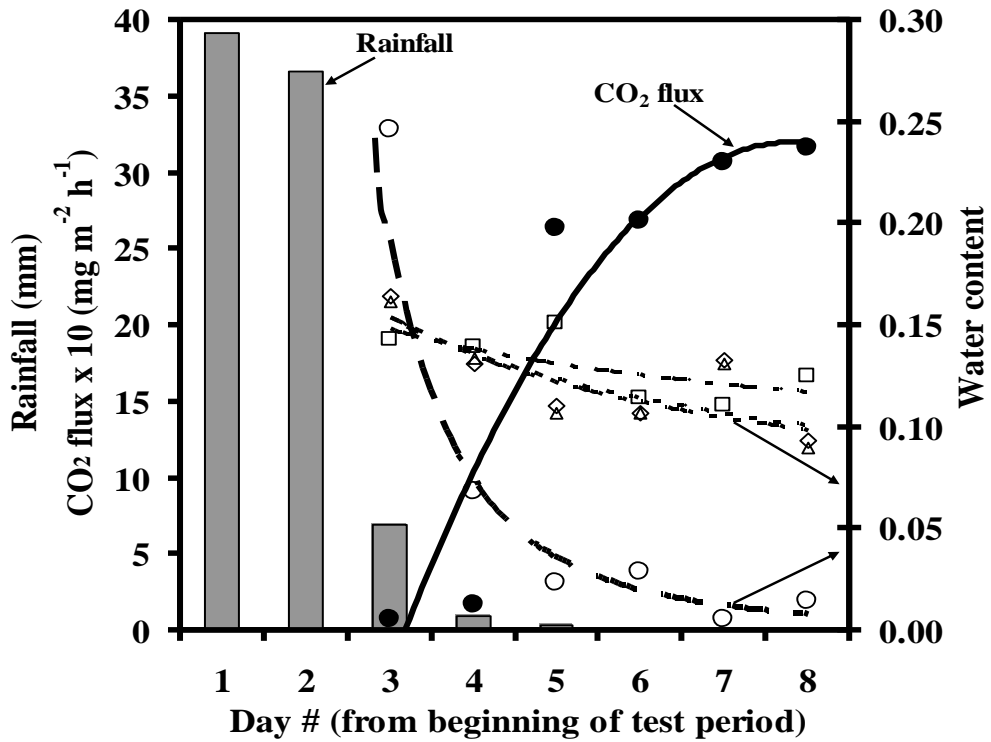
Figure 6.  Rainfall  (   ) CO$_2$ flux (-•-)  and  water  contents  [-o- (0 m); -□- (0.05 m); -Δ- (0.10 m); -◊- (0.15 m)] measured over an 8-d test period [July 29 (day 1) to 5 August (day 8), 2002] at the Deilmann north waste-rock pile (DNWR).



Figure 7A.  Picture showing the Deilmann north waste-rock pile (DNWR).



Figure 7B.  Picture showing the ground surface of the DNWR after heavy rainfall events
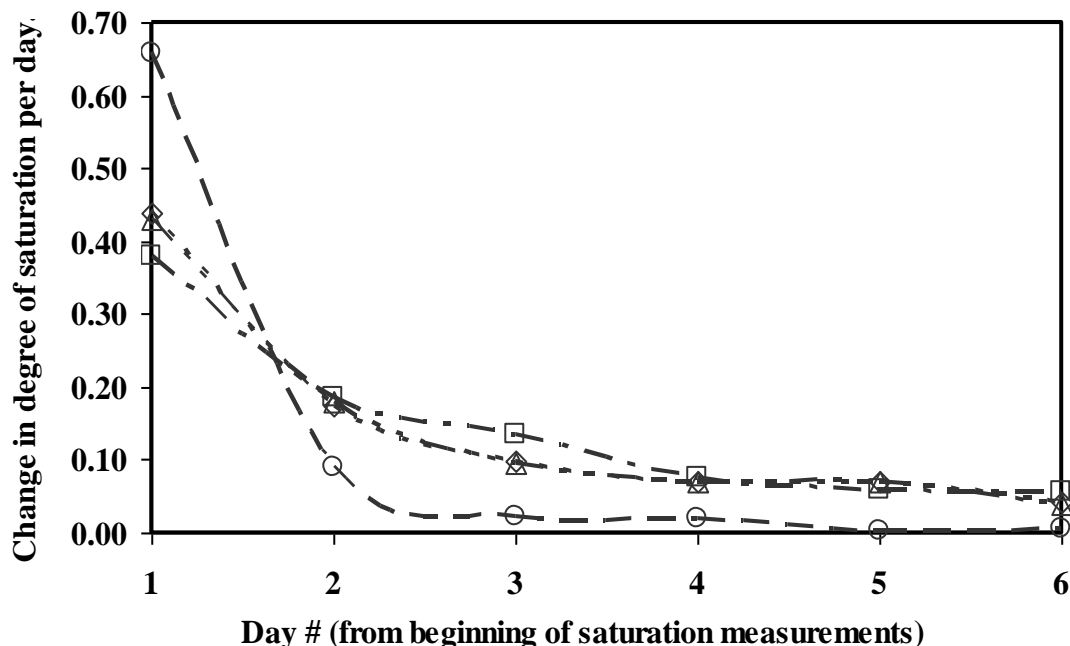
Figure 8. Changes in degree of saturation per day of (i) the surface (-o-, 0 m) and (ii) deeper depths (-□-, 0.05 m; -Δ-, 0.10 m; -◊-, 0.15 m) measured over an 8-d test period [29 July (day 1) to 5 August (day 8), 2002] at the Deilmann north waste-rock pile (DSWR).

Capehart and Carlson (1994) assumed that a shallow drying layer was formed as the rate of drying increases near the surface and decreases below the drying layer at depths > 0.05 m, thereby capping the water loss in the soil and reducing soil evaporation. Hillel (1980) noted that continuation of the drying (evaporation) process for a prolonged period is sometimes accompanied by the development of a distinct desiccated zone, through which water can move from the still-moist underlying layers only by vapor diffusion. Wilson et al. (1994) also noted that the thickness of the dry surface zone increased to form a distinct drying front approximately 0.5 cm thick after 11 or 12 days of column drying and the rate of decline in the evaporation rate appeared to decrease after this point in time.

Short-Term Effects of Rainfall Events on $CO_2$ Gas Efflux from the DNWR

The changes in surface $CO_2$ efflux were also measured during the 8-d test period [29 July (day 1) to 5 August, 2002 (day 8)] at the DNWR except on day 1 and day 2. Results are also presented in Fig. 6 (solid line with solid circles) along with rainfall events and changes in soil water contents. On day 3 (31 July, 2002), the $CO_2$ efflux measured from DNWR was 3 % of its initial average values of 217 mg m$^{-2}$ h$^{-1}$. At this stage of near-saturation all the air pathways to the atmosphere in the upper layers of the waste-rock were closed, and hence, the diffusion of the $CO_2$ gas was dramatically reduced in the upper layer of the waste-rock pile. The figure showed that the change of surface $CO_2$ efflux with time was negatively correlated with measured ground surface waste-rock water content. As the water content at the ground surface decreased exponentially, the surface $CO_2$ efflux increased exponentially from about 7 mg m$^{-2}$ h$^{-2}$ (day 3) to about 306 mg m$^{-2}$ h$^{-2}$ (day 8). These inverse linear relationships between the surface water content and the surface $CO_2$ efflux yielded a correlation coefficient of $R^2 = -0.79$. By the end of

the 8-day test period, the surface $CO_2$ efflux had increased by a factor of 45 while the ground surface water content had decreased from 0.2 to 0.0015 and the measured $CO_2$ gas efflux approximated its initial mean flux value. This observation suggested that it takes about five to six days after a heavy rainfall event for the gas efflux to approach pre-rainfall values at the DNWR. This further suggested that the impact of rainfall events on $CO_2$ effluxes from the waste-rock pile is of relative short duration. In summary, results showed that the surface $CO_2$ efflux is sensitive to changes of waste-rock surface water content after heavy rainfall events, exhibiting a power $(F_{CO2)} = a*\theta_w^{-b} = 1.78*\theta_w^{-1.15}$, $R^2 = 0.79$) decrease with surface water content. The transient effects were attributed to rapid drainage and evaporation. The constants a and b are related to the boundary conditions and conductance properties of the soil. The exponent b which is related to soil diffusivity, is obviously most important, and the greater its value, the greater the decrease in water content.

Short-Term Prediction of Evaporative Fluxes on the DNWR using SoilCover Model

Figure 10 shows the cumulative evaporation predicted by the SoilCover (1997) for the 8-d test period (29 July to 5 August, 2002) at the DNWR during which 75.8 mm rainfall fell over the first 48-h. The SoilCover simulation of evaporation was based on the use of actual weather data (radiation, air temperature, humidity, and wind speed, etc.) and soil physical properties of the test site as inputs. The model permits the calculation of evaporation, both potential (PE) and actual (AE), as a resultant of the interaction between weather and soil factors. The simulation results show that during the early stage of drying following the cessation of the heavy rainfall events the cumulative AE is approximately equal to the cumulative PE from day 3 to day 5 (Fig. 10). The AE started falling progressively below the PE after day 6.
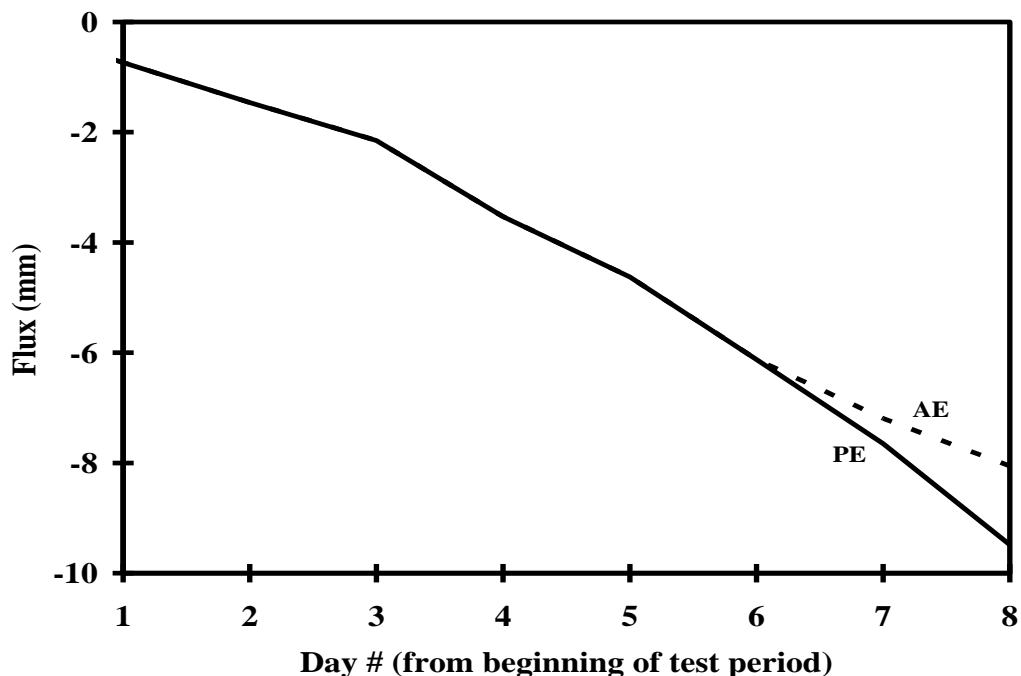


Figure 10. Simulated cumulative actual evaporation (AE) and potential evaporation (PE) for an 8-day test period [29 July (day 1) to 5 August (day 8), 2002] on the Deilmann north waste-rock pile (DNWR) using SoilCover model.

It should also be noted that the transition from stage II to stage III drying occurred from day 5 to day 6 when the ground surface became desiccated and its water content dropped to its lowest value of about 0.001 (see Figs. 6 and 8). Similarly the separation of the AE from PE may signals the transition from stage II to stage III drying. At the end of the test period (day 8) the ratio of PE/AE was 1.25. Wilson et al. (1994) noted that the formation of a dry soil surface was important, as it signals the rapid decline in evaporative flux and the transition to vapor diffusion.

## Conclusions

In a previous study the DCC method was used to determine the magnitude of spatial and, to lesser degree, temporal variations in the $CO_2$ efflux at the DNWR (Kabwe et al. 2005, 2005b). In the current study, we investigated the effects of heavy rainfall events on the near surface water contents and the resultant $CO_2$ efflux. Results showed that the $CO_2$ gas efflux was dramatically reduced after heavy rainfall events but the impact was of relative short duration. Results also showed that at higher degree of saturation the drying of the surface layer (0 m) and those at deeper depths (0.05 – 0.15 m) were proceeding at different rates but more rapidly at the ground surface. But when the ground surface became desiccated the slopes of all the drying lines were approximately similar. The simulated results using SoilCover model showed that the AE fell below the PE once the ground surface became desiccated. The average $O_2$ flux into the DNWR was estimated using the measured $CO_2$ effluxes (average $CO_2$ flux of 217 mg m$^{-2}$ h$^{-1}$) (Kabwe et al., 2005b) and the reported kinetic ratio ($1O_2$:$0.2CO_2$) (Lee et al., 2003) determined from samples collected from the DNWR and was calculated to be 789 mg m$^{-2}$ h$^{-1}$. This study should be of value in the development of a long-term management plan for waste-rock piles.

## Acknowledgements

## Literature Cited

Affek, H., Ronen, D., Yakir, D., 1998. Production of CO2 in the capillary fringe of a deep phreatic aquifer. Water Resour. Res. 34 (5), 989-996. http://dx.doi.org/10.1029/98WR00095.

Ahuja, L.R., Ross, J.D., Bruce, R.R., and Cassel, D.K. 1988. Determining unsaturated Hydraulic conductivity from tensiometric data alone. Soil Sci. Soc. Am. J. 52: 27-34. http://dx.doi.org/10.2136/sssaj1988.03615995005200010005x.

Aggarwal, P.K., Fuller, M.E., Gurgas, M.M., Manning, J.F., Dillon, M.A. 1977. Use os stable oxygen and carbon dioxide isotope analyses for monitoring the pathways and rates of intrinsic and enhanced in situ biodegradation. Environ. Sci. Technol. 31: 590-596. http://dx.doi.org/10.1021/es960562b.

Aggarwal, P.K., Dillon, M.A., 1998. Stable isotope composition of molecular oxygen in soil gas and ground-water: a potentially robust tracer for diffusion and oxygen consumption processes. Geochim. Cosmochim. Acta 62 (4): 577-584). http://dx.doi.org/10.1016/S0016-7037(97)00377-3

Alexander, M., 1977. Introduction to Soil Microbiology, 2$^{nd}$ ed. Wiley, New York. 467 pp.

Amundson. R.G., Chadwick, O.A., Sowers, J.M., Doner, H.E., 1988. Relationship between climate and vegetation and the satble carbon isotope chemistry of soils in the eastern Mojave desert. Nevada. Quat. Res. 29: 245-254. http://dx.doi.org/10.1016/0033-5894(88)90033-6

Barbour, S.L. 1998. Nineteenth Canadian Geotechnical Colloquium: The soil-water characteristic curve: a historical perspective. Can. Geotech. J. 35(5): 873-894. http://dx.doi.org/10.1139/t98-040.

Birkham, T.K. M.Sc. Dissertation, University of Saskatchewan, 2002.

Birkham, T.K., Hendry, M.J., Wassenaar, L.I., Mendoza, C.A., and Lee, E.S. 2003. Characterizing Geochemical Reactions in Unsaturated Mine Waste-Rock Piles Using Gaseous O2, CO2, 12CO2, and 13CO2. Environ. Sci. Technol. 37: 496-501. http://dx.doi.org/10.1021/es020587c.

Brooks, R.H., and Corey, A.T. 1964. Hydraulic properties of porous media. Hydrology Paper, No. 3, Colorado State University, Fort Collins, Colorado.

Capehart, W.J., and Carlson, T.N. 1994. Estimating near-surface soil-moisture availability using a meteorologically driven soil water profile model. J. Hydrol. 160(1-4): 1-20. http://dx.doi.org/10.1016/0022-1694(94)90031-0.

Davidson, J.M., Stone, L.R., Nielsen, D.R., and Larue, M.E. 1969. Field measurement and use of soil-water properties. Water Resour. Res. 5: 1312-1321. http://dx.doi.org/10.1029/WR005i006p01312.

Drake, J.A., Huxel, G.R., Hewitt, C.L., 1996. Microcosms as models for generating and testing community theory. Ecology 77, 670-677. http://dx.doi.org/10.2307/2265489.

Drever, J.I., 1997. the Geochemistry of Natural Waters, 3$^{rd}$ ed. Prentice Hall. Upper Saddle River, NJ. 436 pp.

Elberling, B., and Nicholson, R.V. 1996. Field determination of sulfide oxidation rates in mine tailings. Water Resour. Res. 32: 1773-1784. http://dx.doi.org/10.1029/96WR00487.

Fredlund, D.G., and Rahardjo, H. 1993. Soil mechanics for unsaturated soils. John Wiley & Sons, Inc., New York. http://dx.doi.org/10.1002/9780470172759.

Fredlund, D.G., and Xing, A. 1994. Equations for the Soil-Water Characteristic Curve. Can. Geotech. J. 31: 521-532. http://dx.doi.org/10.1139/t94-061.

Freeze, R.A. 1969. The mechanism of natural ground-water recharge and discharge 1. One-dimensional, vertical, unsteady, unsaturated flow above a recharging ground-water flow system. Water Resour. Res. 5(1): 153-171. http://dx.doi.org/10.1029/WR005i001p00153.

Gardner, W.R. 1956. Calculation of capillary conductivity from pressure plate outflow data. Soil Sci. Soc. Am. Proc. 20: 317-320. http://dx.doi.org/10.2136/sssaj1956.03615995002000030006x.

Gray, D.M. 1995. Handbook of Hydrology, University of Saskatchewan, Saskatoon, SK, Canada.

Grice, G., Reeve, M., 1982. Marine Mesocosms: Biological and Chemical research in Experimental Ecosystems Springer-Verlag, New York. 430 pp.

Hass, H., Fisher, D.W., Thorstenson, D.C., Weeks, E.P. 1983. 13CO$_2$ and 14CO$_2$ measurements on soil atmosphere sampled in the subsoil unsaturated zone in the westerm Gread Plains of the U.S. Radiocarbon **25**: 301-314. https://doi.org/10.1017/S0033822200005610

Hendry, M.J., Lawrence, J.R., Zanyk, B.N., Kirkland, R. 1993. Mircobial production of CO2 in unsaturated geologic media in a mesoscale model. Water Resour. Re. 29: 973-984. http://dx.doi.org/10.1029/92WR02847.

Hendry, M.J., Mendoza, C.A., Kirkland, R.A., Lawrence, J.R., 1999. Quantification of transient CO2 production in a sandy unsaturated zone. Water Resour. Res. 35 (7), 2189-2198. http://dx.doi.org/10.1029/1999WR900060.

Hendry, M.J., Mendoza, C.A., Kirkland, R., Lawrence, J.R., 2001. An assessment of a mesocosm approach to the study of microbial respiration in a sandy unsaturated zone. Groundwater 39 (3), 391-400. http://dx.doi.org/10.1111/j.1745-6584.2001.tb02323.x.

Hillel, D. 1980. Applications of Soil Physics, Academic Press, Inc., New York.

Huang, S., Barbour, S.L., and Fredlund, D.G. 1998. Development and verification of a coefficient of permeability function for a deformable unsaturated soil. Can. Geotech. J. 35: 411-425. http://dx.doi.org/10.1139/t98-010

Kabwe, K.L., Hendry, M.J., Wilson, G.W., and Lawrence, J.R. 2002. Quantifying CO2 fluxes from soil surfaces to the atmosphere. J. Hydrol. 260: 1-14. http://dx.doi.org/10.1016/S0022-1694(01)00601-1.

Kabwe, K.L., Farrell, R.E., Carey, S.K., and Hendry, and Wilson, G.W. 2005. Characterizing Spatial and Temporal Variations in CO2 Fluxes from Surface Using Three Complimentary Measurement Techniques. J. Hydrol. 311: 80-90. http://dx.doi.org/10.1016/j.jhydrol.2004.12.015.

Kabwe, K.L., Wilson, G.W., and Hendry, M.J. 2005b. Effects of Rainfall Events on Waste-Rock Surface Water Conditions and CO2 Effluxes Across the Surfaces of two Waste-Rock Piles. J. Environ. Eng. Sci. 4: 1-12. http://dx.doi.org/10.1139/s05-008.

Keller, C.K., Bacon, D.H., 1998. Soil respiration and georespiration disctinguished by transport analyses of vadose CO2, 13CO2, and 14CO2. Glob. Biogeochem. Cycles 12(2), 361-372. http://dx.doi.org/10.1029/98GB00742.

Key Lake Mining Corporation 1979. Environmental Impact Statement for the Key Lake Project.

Lawrence, J.R., Hendry, M.J., 1995. Mesocosms for subsurface research. Water Qual. Res. J, Can. 30 (3), 493-512.

Lee, E.S., Hollings, P., and Hendry, M.J. 2003b. Use of O2 consumption and CO2 production in kinetic cells to delineate pyrite oxidation-carbonate buffering and microbial respiration in unsaturated media. J. Cont. Hydro. 65: 203-217. http://dx.doi.org/10.1016/S0169-7722(02)00248-6.

Lundgren, A., 1985. Model ecosystems as a tool in freshwater and marine research. Arch. Hydrogiol., Suppl. 70, 157-196.

Mualem, Y. 1978. Hydraulic conductivity of unsaturated porous media: generalized macroscopic approach. Water Resour. Res. 14: 325-334. http://dx.doi.org/10.1029/WR014i002p00325.

Noel, M., M., Rykaart, E.,M 2003. Comparative Study of Surface Flux Boundary Models to Design Soil Covers for Mine Waste Facilities. 6th ICARD, Cairns, QLD, 12-18 July 2003.

Osozawa, S., and Hasegawa, S. 1995. Dial and Seasonal changes in carbon dioxide concentration and flux in an Andisol. Soil Sci. 160: 117-124. http://dx.doi.org/10.1097/00010694-199516020-00005.

Philip, J.R. 1986. Linearized unsteady multidimentional infiltration. Water Resour. Res. 22: 1717-1727. http://dx.doi.org/10.1029/WR022i012p01717.

Pritchard, D.T., and Curie, J.A. 1982. Diffusion of coefficients of carbon dioxide, nitrous oxide, ethylene and ethane in air and their measurement. Soil Sci. 33: 175-184. http://dx.doi.org/10.1111/j.1365-2389.1982.tb01757.x.

Richards, L.A. 1931. Capillary conduction of liquid through porous medium. Journal of Physics 1: 318-333. http://dx.doi.org/10.1063/1.1745010.

Richards, J. 1997. Waste rock investigations: Key Lake operation final report for Cameco Corporation. Department of Geological Sciences, University of Saskatchewan, Saskatoon, Saskatchewan. 18 pp.

Ritchie, A.I.M. 1994. Short Course Handbook on Environmental Geochemistry of sulfide Mine-Wastes; Jambor, L., Blowes, D. W., Eds.; Mineralogical Association of Canada: Waterloo, Ontario, 1994.

SoilCover, 1997. SoilCover User's Manual, Unsaturated Soils Group, Department of Civil Engineering, University of Saskatchewan, Saskatoon, Saskatchewan, Canada.

Solomon, D.K., Cerling, T.E. 1987. The annual carbon dioxide cycle in a montaine soil: observations, modeling, and implications for weathering. Water Resour. Res. 23 (12): 2257-2265. http://dx.doi.org/10.1029/WR023i012p02257.

Thorstenson, C.D., Weeks, E.P., Haas, H., Fisher, D.W. 1983. Distribution of gaseous $12CO_2$, $13CO_2$, and $14CO_2$ in the subsoil unsaturated zone of the western Great Plains of the U.S. Radiocarbon **25**: 315-346. https://doi.org/10.1017/S0033822200005622

Timms, G.P., and Bennet, J.W. 2000. In Proceeding of the international conference on acid rock drainge, Denver, Colorado 2000: 841-849.

Wang, Y., Amundson, R., Trumbore, S. 1999. The impact of land use change on C turnover in soils. Glob. Biogeochem. Cycles 13(1): 47-57. http://dx.doi.org/10.1029/1998GB900005.

Wilson, G.W. 1990. Soil Evaporative Fluxes for Geotechnical Engineering Problems. Ph.D. Thesis, University of Saskatchewan, Saskatoon, Saskatchewan, Canada.

Wilson, G.W., Fredlund, D.G., and Barbour, S.L. 1994. Coupled soil-atmosphere modeling for soil evaporation. Can. Geotech. J. 31: 151-161. http://dx.doi.org/10.1139/t94-021.

Wind, G.P. 1955. Field experiment concerning capillary rise of moisture in heavy clay soil. Netherlands Journal of Agricultural Science **3**: 60-69.

Wood, B.D., Petraitis, M.J. 1984. Origin and distribution of carbon dioxide in the unsaturated zone of the southern High Plains of Texas. Water Resour. Res. 20 (9): 1193-1208. http://dx.doi.org/10.1029/WR020i009p01193.

Wood, B.D., Keller, C.K., Johnston, D.L.,1993. In situ measurements of microbial activity controls on microbial CO2 production in the unsaturated zone. Water Resour. Res. 29 (3), 647-659. http://dx.doi.org/10.1029/92WR02315